Consistency of spectroscopic factors from $(e,e'p)$ reactions at different momentum transfers

Marco Radici
Dipartimento di Fisica Nucleare e Teorica, Università di Pavia
and Istituto Nazionale di Fisica Nucleare, Sezione di Pavia, I-27100 Pavia, Italy

W.H. Dickhoff
Department of Physics, Washington University, St. Louis, Missouri 63130

E. Roth Stoddard
Department of Physics, University of Missouri at Kansas City, Kansas City, Missouri 64110
(Received 14 March 2002; published 24 July 2002)

The possibility to extract relevant information on spectroscopic factors from $(e,e'p)$ reactions at high Q^2 is studied. Recent ^{16}O$(e,e'p)$ data at $Q^2=0.8$ $(\mathrm{GeV}/c)^2$ are compared to a theoretical approach that includes an eikonal description of the final-state interaction of the proton, a microscopic nuclear matter calculation of the damping of this proton, and high-quality quasihole wave functions for *p*-shell nucleons in ^{16}O. Good agreement with the $Q^2=0.8$ $(\mathrm{GeV}/c)^2$ data is obtained when spectroscopic factors are employed that are identical to those required to describe earlier low-Q^2 experiments.

DOI: 10.1103/PhysRevC.66.014613 PACS number(s): 25.30.Dh, 21.10.Jx, 24.10.Jv

I. INTRODUCTION

During the last fifteen years a quiet revolution has taken place in the perception of the nucleus. During this period the study of the $(e,e'p)$ reaction has clarified the limits of validity of the mean-field description of nuclei. In particular, absolute spectroscopic factors have been obtained for the removal of protons from many nuclei [1–4]. The qualitative features of the strength distribution suggest a considerable mixing between single-hole states and more complicated configurations, such as two-hole–one-particle states. The resulting fragmentation pattern of the single-particle (SP) strength exhibits a single peak carrying about 65–70 % of the strength for states in the immediate vicinity of the Fermi energy, while more deeply bound orbitals display a strongly fragmented distribution reminiscent of a complex SP energy. In addition to these fragmentation features, an important depletion of the SP strength has been established that is associated with ground-state correlations induced by strong short-range and tensor correlations [5]. This leads to an overall reduction of the SP strength for all mean-field orbits in all nuclei by 10–15 % [6,7]. This theoretical result has recently been confirmed also for deeply bound orbits in an $(e,e'p)$ experiment on ^{208}Pb in a wide domain of missing energy and momentum [8,9].

The analysis of the $(e,e'p)$ data has relied on the distorted wave impulse approximation (DWIA) for both the Coulomb distortion of the electron waves (in heavy nuclei) and the outgoing proton [10–13]. The proton distortion is described in terms of an optical potential required to describe elastic proton scattering data at relevant energies [3]. There is some uncertainty related to this treatment since elastic proton scattering is considered to be a surface reaction and no detailed information is obtained related to the interior of the nucleus. This uncertainty gives rise to an estimated error of about 10%. Such an estimate may be inferred by considering the difference between the relativistic and nonrelativistic treatment of the proton distortion. It is shown in Ref. [14] that this difference is essentially due to the reduction of the interior wave function in the relativistic case. This feature can also be generated by including a reasonable amount of nonlocality in the optical potential [14].

A serious challenge to the interpretation of $(e,e'p)$ experiments was recently published in Refs. [15,16]. This challenge consists of questioning the validity of the constancy of the spectroscopic factor as a function of the four-momentum (squared), Q^2, transferred by the virtual photon to the knocked-out nucleon. In Ref. [15] a conventional analysis of the world's data for $(e,e'p)$ experiments on ^{12}C at low Q^2 generated results consistent with previous expectations. Data at higher values of Q^2 were then analyzed within the framework of a theoretical model that employs Skyrme-Hartree-Fock bound-state wave functions for the initial proton, a Glauber-type description of the final-state interaction of the outgoing proton, and a factorization approximation for the electromagnetic vertex [15,16]. Within the framework of this theoretical description, spectroscopic factors were obtained that increase substantially with increasing Q^2 for the ^{12}C nucleus.

The spectroscopic factor is a many-body quantity defined without reference to a probe. For valence hole states in nuclei it simply represents the probability for the removal of a nucleon with prescribed quantum numbers from the ground state of the target while ending up in a state of the nucleus with one particle less. In the conventional analysis of the experimental data these quantum numbers involve the trivial values of parity and total angular momentum but also require the corresponding wave function to be a solution of a Woods-Saxon potential at the appropriate binding energy. This potential is adjusted to generate an optimum description of the shape of the experimental cross section. The resulting theoretical representation of the cross section must then be multiplied by a constant factor to coincide with the experimental cross section. This constant factor is then interpreted

as the spectroscopic factor. Another important ingredient in this analysis is the choice of the electron-proton cross section, which must be considered off-shell [17]. This leads to a small additional uncertainty in the analysis of low Q^2 data as discussed recently in Ref. [18].

Further clarification of this intriguing situation with different spectroscopic factors at different Q^2 is urgently needed. For this purpose we consider in this paper a study of recently published $(e,e'p)$ data for ^{16}O at $Q^2=0.8$ $(\mathrm{GeV}/c)^2$ [19]. An unfactorized approach is used, as it is required at low Q^2 [11] and has been recently advocated also for high Q^2 reactions in Ref. [20]. However, the higher energy of the outgoing proton requires a description that contains different elements than the conventional low-Q^2 analysis. For the electromagnetic current operator we follow the approach of Ref. [21], where a relativistic current operator was used in a Schrödinger-based calculation, avoiding any nonrelativistic reduction and including the effect of spinor distortion by the Dirac scalar and vector potentials (see also Refs. [22–25,14]). As for the final state, we employ a recently developed eikonal description of the final-state interaction (FSI) of the proton with the nucleus that has been tested against DWIA solutions of a complex spin-dependent optical potential [26,27]. The absorption of the proton is described theoretically by linking it to the corresponding absorption of a nucleon propagating through nuclear matter. The relevant quantity is the nucleon self-energy, which is obtained from a self-consistent calculation of nucleon spectral functions including the effects of realistic short-range and tensor correlations [28]. This description of the FSI is combined with previous results for the bound-state wave functions of the *p*-shell quasihole states in ^{16}O [29], which have been deduced by solving the Dyson equation with a nucleon self-energy containing the same short-range correlations but in a finite volume. In Ref. [30] these wave functions have been used to analyze low-Q^2 data for the $^{16}\mathrm{O}(e,e'p)$ reaction [31]. In the present work, these very same wave functions produce a good description of the shape of the coincidence cross section for the *p*-shell quasihole states at high-Q^2 [19] using the same spectroscopic factors obtained from the low-Q^2 data [31]. A preliminary result was reported in Ref. [32].

A consistent analysis of low- and high-Q^2 data requires an approach in which the same quasihole wave functions and corresponding spectroscopic factors are used in both cases. In this paper we present such an approach. In Sec. II we discuss the ingredients of the theoretical description including the structure of the electromagnetic current (Sec. II A), the eikonal approximation (Sec. II B), and the final hadronic tensor (Sec. II C). The many-particle ingredients are discussed in Sec. III, which includes a summary of the calculation of the quasihole wave functions in Sec. III A, a description of the construction of the nonlocality factor required by a treatment of relativistic effects in Sec III B, and, finally, an overview of the ingredients to describe the damping of high-momentum protons in nuclear matter (Sec. III C). The results are discussed in Sec. IV while final conclusions are drawn in Sec. V.

II. THE MODEL

In the one-photon exchange approximation, the differential cross section for the scattering of an ultrarelativistic electron with initial (final) momentum $\vec{p}_e$ $(\vec{p}\,'_e)$, off a nuclear target from which a nucleon is ejected with final momentum $\vec{p}\,'_N$, reads [10–12]

$$\frac{d\sigma}{d\vec{p}\,'_e d\vec{p}\,'_N}=\frac{e^4}{16\pi^2}\frac{1}{Q^4 p_e p'_e}\sum_{\lambda,\lambda'=0,\pm1} L_{\lambda,\lambda'}W_{\lambda,\lambda'}, \qquad (1)$$

where $Q^2=q^2-\omega^2$ and $\vec{q}=\vec{p}_e-\vec{p}\,'_e$, $\omega=p_e-p'_e$ are the momentum and energy transferred to the target nucleus, respectively. The lepton tensor $L_{\lambda,\lambda'}$ and hadron tensor $W_{\lambda,\lambda'}$ are conveniently expressed in the basis of unit vectors

$$e_0=(1,0,0,0), \quad e_{\pm1}=\left(0,\mp\sqrt{\frac{1}{2}},-\sqrt{\frac{1}{2}}i,0\right), \qquad (2)$$

which define the longitudinal (0) and transverse (±1) components of the nuclear response with respect to the polarization of the exchanged virtual photon. The hadron tensor is defined as [10,11,13]

$$W_{\lambda,\lambda'}=(-1)^{\lambda+\lambda'}e^{\mu}_{\lambda}e^{\nu *}_{\lambda'}\overline{\sum_i}\sum\!\!\!\!\!\!\int_f J_\mu J^*_\nu \delta(E_f-E_i-\omega), \qquad (3)$$

i.e., it involves the average over initial states and the sum over the final undetected states (compatible with energy-momentum conservation) of bilinear products of the scattering amplitude J^μ.

This basic ingredient of the calculation is built from the matrix element of the nuclear charge-current density operator $\hat{J}^\mu$ between the initial, $|\Psi^A_0\rangle$, and the final, $|\Psi^A_f\rangle$, nuclear states. This complicated *A*-body problem can be simplified by projecting out of the Hilbert space the specific channel that corresponds to the experimental asymptotic conditions of a knocked-out nucleon with momentum $\vec{p}\,'_N$ and of a residual nucleus, recoiling with momentum $-\vec{p}_m=\vec{q}-\vec{p}\,'_N$ and mass M_R, in a well-defined state $|\Psi^{A-1}_n(E_R)\rangle$ with energy E_R and quantum numbers *n*. The scattering amplitude can be rewritten in a one-body representation (in momentum space and omitting spin degrees of freedom for simplicity) as [11,33]

$$J^\mu_n(\omega,\vec{q},\vec{p}\,'_N,E_R)=\int d\vec{p}\,d\vec{p}\,'\,\chi^{(-)*}_{\vec{p}\,'_N E_R n}(\vec{p}\,')\hat{J}^\mu_{\mathrm{eff}}(\vec{p},\vec{p}\,',\vec{q},\omega) \times\phi_{E_R n}(\vec{p})[S_n(E_R)]^{1/2}, \qquad (4)$$

provided that $\hat{J}^\mu$ is substituted by an appropriate effective one-body charge-current density operator $\hat{J}^\mu_{\mathrm{eff}}$, which guarantees the orthogonality between $|\Psi^A_0\rangle$ and $|\Psi^A_f\rangle$ besides taking into account effects due to truncation of the Hilbert space. Usually, the orthogonality defect is negligible in standard kinematics for $(e,e'p)$ reactions [10,11,33]; in any

case, $\hat{J}^{\mu}_{\rm eff}$ is here approximated by a one-body relativistic current operator including spinor distortion along the lines described in the following Sec. II A.

The functions

$$[S_n(E_R)]^{1/2}\phi_{E_R n}(\vec{p})=\langle\Psi_n^{A-1}(E_R)|a(\vec{p})|\Psi_0^A\rangle,$$

$$\chi^{(-)}_{p'_N E_R n}(\vec{p})=\langle\Psi_n^{A-1}(E_R)|a(\vec{p})|\Psi_f^A\rangle, \tag{5}$$

describe the overlap between the residual state $|\Psi_n^{A-1}(E_R)\rangle$ and the hole produced in $|\Psi_0^A\rangle$ and $|\Psi_f^A\rangle$, respectively, by removing a particle with momentum $\vec{p}$. Both $\phi_{E_R n}$ and $\chi^{(-)}_{p'_N E_R n}$ are eigenfunctions of a Feshbach-like nonlocal energy-dependent Hamiltonian referred to the residual nucleus, belonging to the eigenvalues E_R and $E_R+\omega$, respectively [34,11]. The norm of $\phi_{E_R n}$ is 1 and $S_n(E_R)$ is the spectroscopic factor associated with the removal process, i.e., it is the probability that the residual nucleus can indeed be conceived as the target nucleus with a hole. The dependence of $\chi^{(-)}_{p'_N E_R n}$ upon p'_N is hidden in the asymptotic state $|\Psi_f^A\rangle$ and the boundary conditions are those of an incoming wave.

Because of the complexity of the eigenvalue problem in the continuum, a complex mean-field interaction with energy-dependent parameters is usually assumed between the residual nucleus and the emitted nucleon. Then, $\chi^{(-)}_{p'_N E_R n}\sim\chi^{(-)}_{p'_N}$ and the nonlocality of the original Feshbach Hamiltonian is taken into account by multiplying the scattering wave by the appropriate Perey factor [35]. Several models for this FSI are discussed in the literature (for a review, see Refs. [11,12]). Here, the eikonal approximation is adopted and is described in more detail in Sec. II B. Finally, in Sec. II C we present the complete formula for the hadronic tensor used in the calculation.

A. Current operator and spinor distortion

While new data for the $(e,e'p)$ reaction have become available at very high proton energies [19,36,37], it has also become evident that many ingredients of the theoretical calculations must be upgraded and made adequate for the new kinematical regime. In particular, a nonrelativistic reduction of the electromagnetic current operator is no longer reliable. Since all other ingredients entering the scattering amplitude will be deduced in a Schrödinger-like framework, we follow the approach of Ref. [21].

It is well known that a four-component Dirac spinor Ψ, with positive- and negative-energy components ψ_+ and ψ_-, respectively, satisfying a Dirac equation with energy eigenvalue E, mass m, scalar and vector potentials S and V, respectively, can be written as

$$\Psi=\begin{pmatrix}\psi_+\\ \psi_-\end{pmatrix}=\sqrt{\frac{E+m}{2m}}\begin{pmatrix}1\\ \dfrac{\vec{\sigma}\cdot\hat{\vec{\pi}}}{E+m+S(r)-V(r)}\end{pmatrix}D^{1/2}(r)\phi$$

$$\equiv\Lambda(\hat{\vec{\pi}},r)\phi, \tag{6}$$

namely, it can be represented by the action of the operator $\Lambda(\hat{\vec{\pi}},r)$ on the wave function ϕ, that satisfies a Schrödinger-equivalent equation with central U_C and spin-orbit U_{LS} potentials, which can either be expressed in terms of S and V or replaced by intrinsically nonrelativistic potentials. The Darwin nonlocality factor

$$D(r)=1+\frac{S-V}{E+m} \tag{7}$$

is related to U_{LS} by

$$U_{LS}(r)=-\frac{1}{2\mu}\frac{1}{rD}\frac{dD}{dr}, \tag{8}$$

where $\mu\sim m(A-1)/A$ is the reduced mass with A the mass number.

In Ref. [21], the calculations were performed in configuration space by defining the effective current operator (omitting spin indices for simplicity)

$$\hat{J}^{\mu}_{\rm eff}=\Lambda^{\dagger}(\vec{p}'_N,r)\gamma^0\Gamma^{\mu}\Lambda(\vec{p}_m,r) \tag{9}$$

and by evaluating the operator part $\vec{\sigma}\cdot\hat{\vec{\pi}}$ in the effective momentum approximation (EMA), i.e., by replacing the operator $\hat{\vec{\pi}}$ with the momenta $\vec{p}'_N,\vec{p}_m$ determined by asymptotic kinematics. After choosing one out of the three (on-shell) equivalent expressions for the electromagnetic vertex function Γ^{μ} [17], the effective current operator $\hat{J}^{\mu}_{\rm eff}$ was reduced to a simple 2×2 matrix acting on the nucleon spins, using the standard representation for γ matrices as 4×4 operators in terms of 2×2 Pauli spin matrices [38].

Here, the scattering amplitude is worked out in momentum space. Therefore, the operator $\vec{\sigma}\cdot\hat{\vec{\pi}}$ becomes just a multiplicative factor with a 2×2 matrix structure in spin space acting on the nucleon spins. Consequently, Eq. (4) can be specialized to a ''relativized Schrödinger framework'' by considering the following effective current operator (omitting again spin indices for simplicity),

$$\hat{J}^{\mu}_{\rm eff}(\vec{p},\vec{p}',\vec{q},\omega)$$

$$=\frac{1}{(2\pi)^3}\int d\vec{r}\,e^{i(\vec{p}+\vec{q}-\vec{p}')\cdot\vec{r}}\Lambda^{\dagger}(\vec{p}',r)\gamma^0\Gamma^{\mu}\Lambda(\vec{p},r), \tag{10}$$

as can be easily shown by starting from the expression of the scattering amplitude in configuration space and applying the proper Fourier transformations. The nonrelativistic limit of Eq. (10) is recovered by setting $E,E'\sim m$, and $S(r)=V(r)=0$. Inspection of Eqs. (7) and (6) indicates that in this limit the spinor-distortion operator no longer depends on r and the

Fourier transform in Eq. (10) produces the well-known $\delta(\vec{p}'-\vec{p}-\vec{q})$ accounting for momentum conservation [10,11]. In the following, we will keep $D(r)=1$ for the scattering state, because the distortion of a high-energy ejectile will be approximated by a uniform damping in nuclear matter with $U_{LS}=0$ (see Sec. II B).

The electromagnetic vertex function Γ^μ for an on-shell nucleon can be represented through three equivalent expressions related by the Gordon identity [17]. Here, we choose the following:

$$\Gamma^\mu=\gamma^\mu G_M(Q^2)-\frac{P^\mu}{2m}F_2(Q^2), \tag{11}$$

where G_M is the nucleon magnetic form factor, F_2 is its Pauli form factor, and $P^\mu=(E'+E,\vec{p}'+\vec{p})$. By inserting Eq. (11) in Eq. (10), the scattering amplitude becomes

$$\begin{aligned}J^\mu_n(\omega,\vec{q},\vec{p}'_N,E_R)&=\int d\vec{p}\,d\vec{p}'\,\chi^{(-)*}_{p'_N E_R n}(\vec{p}\,')\hat{J}^\mu_{\rm eff}(\vec{p},\vec{p}\,',\vec{q},\omega)\,\phi_{E_R n}(\vec{p})[S_n(E_R)]^{1/2}\\&=\int d\vec{p}\,d\vec{p}'\,\chi^{(-)*}_{p'_N E_R n}(\vec{p}\,')\sqrt{\frac{E+m}{2m}}\sqrt{\frac{E'+m}{2m}}\frac{1}{(2\pi)^{3/2}}\left\{G_M(Q^2)\left[\delta_{\mu 0}\left(\hat{D}^{1/2}+\frac{\vec{\sigma}\cdot\vec{p}\,'}{E'+m}\frac{\vec{\sigma}\cdot\vec{p}}{E+m}\hat{D}^{-1/2}\right)\right.\right.\\&\left.\left.+\delta_{\mu i}\left(\vec{\sigma}\frac{\vec{\sigma}\cdot\vec{p}}{E+m}\hat{D}^{-1/2}+\frac{\vec{\sigma}\cdot\vec{p}\,'}{E'+m}\vec{\sigma}\hat{D}^{1/2}\right)\right]-\frac{P^\mu}{2m}F_2(Q^2)\left[\hat{D}^{1/2}-\frac{\vec{\sigma}\cdot\vec{p}\,'}{E'+m}\frac{\vec{\sigma}\cdot\vec{p}}{E+m}\hat{D}^{-1/2}\right]\right\}\phi_{E_R n}(\vec{p})[S_n(E_R)]^{1/2},\end{aligned} \tag{12}$$

where

$$\hat{D}^{\pm 1/2}\equiv\frac{1}{(2\pi)^{3/2}}\int d\vec{r}\,e^{i(\vec{p}+\vec{q}-\vec{p}\,')\cdot\vec{r}}D^{\pm 1/2}(r) \tag{13}$$

are functions of $|\vec{p}+\vec{q}-\vec{p}\,'|$. The nucleon form factors are taken from Ref. [39], while the Coulomb gauge is adopted to restore current conservation at the one-body level by modifying the longitudinal component accordingly.

B. The eikonal approximation

Similar to the case of current operators, the high proton energies that can be reached in $(e,e'p)$ reactions at the new experimental facilities also demand a suitable approach to the treatment of the proton scattering wave. Traditionally, the assumed mean-field interaction between the ejectile and the residual nucleus has been described by complex spin-dependent optical potentials with energy-dependent parameters constrained by fitting phase shifts and analyzing powers of elastic (inelastic) (p,p) scatterings on the corresponding residual nucleus. A Schrödinger equation with incoming wave boundary conditions for each partial wave of $\chi^{(-)}_{p'_N}$ is solved up to a maximum angular momentum $L_{\max}(p'_N)$ satisfying a convergency criterion. Typically, this method has been successfully applied to $(e,e'p)$ reactions at proton momenta below 0.5 GeV/c and $L_{\max}<50$ [11,12].

At higher energies, the optical analysis of proton elastic scattering is improved by the relativistic description via Dirac phenomenology. The scattering wave is still expanded in partial waves, but each component solves the Dirac equation containing the scalar and vector Dirac potentials [40].

An alternative, simpler but powerful, method by Glauber [41] suggests that, when the proton is highly energetic, the Schrödinger equation is reduced to a first-order differential equation along the propagation axis $\hat{z}$,

$$\left(\frac{\partial}{\partial z}-ip'_N\right)\chi=\frac{i}{2p'_N}U\chi, \tag{14}$$

with boundary conditions such that asymptotically $\chi\to 1$, i.e., corresponding to an incoming unitary flux of plane waves. In the pure Glauber model, $U(r)$ is determined in a parameter-free way starting from the elementary free proton-nucleon scattering amplitude at the considered energy and then averaging over all possible configurations of the spectator nucleons. For $p'_N\gtrsim 1$ GeV/c, the scattering amplitude is dominated by inelastic processes and $U(r)$ is supposed to be mostly sensitive to its imaginary part describing the absorption [42,43,27]. Moreover, the Glauber model predicts that the ratio between the real and imaginary parts of $U(r)$ equals the ratio between the real and imaginary parts of the average proton-nucleon forward scattering amplitude, which is expected to be small anyway beyond the inelastic threshold [42]. Therefore, we can safely assume $U(r)\sim iW(r)$. Then, the solution to Eq. (14) looks like [27]

$$\chi^{(-)}_{p'_N}(\vec{r}) = \exp\left(i\vec{p}'_N\cdot\vec{r} + \frac{i}{2p'_N}\int_z^\infty U(\vec{r}_\perp, z')dz' \right)$$
$$= \exp\left(i\vec{p}'_N\cdot\vec{r} - \frac{1}{2p'_N}\int_z^\infty W(\vec{r}_\perp, z')dz' \right)$$
$$\equiv e^{(i\vec{p}'_N\cdot\vec{r})}e^{(-\vec{p}_I\cdot\vec{r})}, \quad (15)$$

i.e., as a plane wave with a damping factor related to the absorption part of the residual interaction.

The reliability of this eikonal approximation (EA), which has a long tradition of successful results in the field of high-energy proton-nucleus elastic scattering [44], has been tested in the context of knockout reactions and in the momentum range of interest here ($0.6 \lesssim q \lesssim 1$ GeV/c) against solutions of the Schrödinger equation with nonrelativistic complex optical potentials up to $L_{\max}=120$ partial waves [26] (see also Ref. [45]). For increasing energies, the EA is supposed to become more and more reliable, despite the actual semirelativistic nature of the approach [41]. Moreover, for emitted protons with outgoing energy beyond the inelastic threshold and initially bound momentum below the Fermi surface ($p_m \lesssim p_{\rm Fermi} \ll p'_N, q$, with $p_{\rm Fermi}$ the target Fermi momentum: the same kinematic conditions of the E89003 experiment at CEBAF [19]), it has been shown that the proton angular distribution can actually be reproduced by representing the scattering wave as a plane wave with an additional damping [43,27]. After all, for a fast moving object the nuclear density can be considered roughly constant (but for a small portion on the surface) and the eikonal wave of Eq. (15) simply corresponds to the solution of a Schrödinger equation inside homogeneous nuclear matter. In the next Sec. III C, a microscopic justification of the damping factor will be given by a detailed description of the link between p_I and the imaginary part of the self-energy of a nucleon moving inside nuclear matter. Here, it is sufficient to say that the main drawback of such an approach is the lack of any spin-orbit effect in FSI [46] and that for sake of simplicity the damping vector will be kept parallel to the wave vector of the scattered particle, i.e., $\vec{p}_I \| \vec{p}'_N$.

The EA of Eq. (15) can be also formulated by saying that the scattering wave is approximated by a plane wave with a complex momentum $\vec{p}_f = \vec{p}'_N + i\vec{p}_I$ and normalized as

$$\chi^{(-)}_{p'_N}(\vec{r}) = e^{(-\vec{p}_I\cdot\vec{R})}e^{(i\vec{p}_f\cdot\vec{r})} = e^{(-\vec{p}_I\cdot\vec{R})}e^{(i\vec{p}'_N\cdot\vec{r}-\vec{p}_I\cdot\vec{r})}, \quad (16)$$

with $\vec{R}$ a constant vector with modulus equal to the nuclear radius. In fact, for a propagation along the $\hat{z}$ axis, the wave enters the nucleus at $\vec{r}=-\vec{R}\equiv(0,0,-R)$ with unitary modulus and leaves it at $\vec{r}=\vec{R}\equiv(0,0,R)$, damped by $e^{-2\vec{p}_I\cdot\vec{R}}$. In order to consider the Fourier transform of Eq. (16), an extended definition of the distribution δ of a complex variable is required. In the Appendix of Ref. [26], it is actually shown that such an extension is possible so that we can define the EA of the scattering wave in momentum space as

$$\chi^{(-)}_{p'_N}(\vec{p}\,') \equiv e^{-\vec{p}_I\cdot\vec{R}}\delta(\vec{p}_f - \vec{p}\,'), \quad (17)$$

where now $\vec{p}\,'$ is a complex vector. The extension of the matrix element of Eq. (12) to the complex plane in $\vec{p}\,'$ is possible if the rest of the integrand is an analytic function asymptotically vanishing for $|\vec{p}\,'|\to\infty$ [26]. It is rather easy to check that, apart from the δ distribution, the integrand of Eq. (12) meets these requirements. Therefore, the scattering amplitude in the EA (also with spin indices explicitly indicated) becomes

$$(J^\mu)_{s'_N n}(\omega,\vec{q},\vec{p}'_N,E_R) \sim e^{-\vec{p}_I\cdot\vec{R}}\int d\vec{p}\langle s'_N|\hat{J}^\mu_{\rm eff}(\vec{p},\vec{p}_f,\vec{q},\omega)|s_n\rangle\phi_{E_R n}(\vec{p})[S_n(E_R)]^{1/2}$$
$$= \frac{e^{-\vec{p}_I\cdot\vec{R}}}{(2\pi)^{3/2}}\sqrt{\frac{E_f+m}{2m}}\int d\vec{p}\,\sqrt{\frac{E+m}{2m}}\phi_{E_R n}(\vec{p})[S_n(E_R)]^{1/2}\Bigg\{ G_M(Q^2)\Bigg[\delta_{\mu 0}\Bigg(\hat{D}^{1/2}\delta_{s'_N s_n}$$
$$+ \langle s'_N|\vec{\sigma}\cdot\vec{p}_f^{\,*}\vec{\sigma}\cdot\vec{p}|s_n\rangle\frac{\hat{D}^{-1/2}}{(E_f+m)(E+m)}\Bigg) + \delta_{\mu i}\Bigg(\langle s'_N|\vec{\sigma}\vec{\sigma}\cdot\vec{p}|s_n\rangle\frac{\hat{D}^{-1/2}}{E+m} + \langle s'_N|\vec{\sigma}\cdot\vec{p}_f^{\,*}\vec{\sigma}|s_n\rangle\frac{\hat{D}^{1/2}}{E_f+m}\Bigg)\Bigg]$$
$$- \frac{p_f^\mu + p^\mu}{2m}F_2(Q^2)\left[\hat{D}^{1/2}\delta_{s'_N s_n} - \langle s'_N|\vec{\sigma}\cdot\vec{p}_f^{\,*}\vec{\sigma}\cdot\vec{p}|s_n\rangle\frac{\hat{D}^{-1/2}}{(E_f+m)(E+m)}\right]\Bigg\}, \quad (18)$$

where $p^\mu=(E,\vec{p})$, $p_f^\mu=(E_f,\vec{p}_f)$, with $E=\sqrt{|\vec{p}|^2+m^2}$, $E_f=\sqrt{|\vec{p}_f|^2+m^2}$, and s'_N, s_n are the projections of the spins of the detected proton and of the residual hole with collective quantum numbers n, respectively. The Fourier transform of the Darwin nonlocality factor, in agreement with Eq. (13), is function of $|\vec{p}+\vec{q}-\vec{p}_f| = \sqrt{|\vec{p}+\vec{q}-\vec{p}'_N|^2+p_I^2}$.

C. Hadronic tensor

After summing over the undetected final states with quantum numbers n of the residual nucleus, the hadron tensor $W_{\lambda,\lambda'}$ in momentum space becomes

$$W_{\lambda,\lambda'}=(-1)^{\lambda+\lambda'}e^{\mu}_{\lambda}e^{\nu *}_{\lambda'}e^{-2\vec{p}_I\cdot\vec{R}}\sum_n \int d\vec{p}\,d\vec{k}\langle s'_N|(\hat{J}_{\rm eff})_\mu(\vec{p},\vec{p}_f,\vec{q},\omega)|s_n\rangle\phi_{E_R n}(\vec{p})\phi^*_{E_R n}(\vec{k})S_n(E_R)\langle s_n|(\hat{J}_{\rm eff})^\dagger_\nu(\vec{k},\vec{p}_f,\vec{q},\omega)|s'_N\rangle$$

$$\equiv(-1)^{\lambda+\lambda'}e^{\mu}_{\lambda}e^{\nu *}_{\lambda'}e^{-2\vec{p}_I\cdot\vec{R}}\int d\vec{p}\,d\vec{k}\langle s'_N|(\hat{J}_{\rm eff})_\mu(\vec{p},\vec{p}_f,\vec{q},\omega)S(\vec{p},\vec{k};E_R)(\hat{J}_{\rm eff})^\dagger_\nu(\vec{k},\vec{p}_f,\vec{q},\omega)|s'_N\rangle, \tag{19}$$

where

$$S(\vec{p},\vec{k};E_R)=\sum_n S_n(E_R)\phi_{E_R n}(\vec{p})|s_n\rangle\langle s_n|\phi^*_{E_R n}(\vec{k}) \tag{20}$$

is the hole spectral function discussed in Sec. III. The isospin indices have been omitted for simplicity and, as before, the summation over n runs over the undetected final states of the residual nucleus that are present at a given excitation energy E_R.

The hole spectral function can be conveniently expanded in partial waves in a SP basis as

$$S(\vec{p},\vec{k};E_R)=\sum_{lj}\sum_{m_l,m'_l}\sum_{m_s,m'_s}(l\,\tfrac{1}{2}\,m_l m_s|jm)(l\,\tfrac{1}{2}\,m'_l m'_s|jm)S_{lj}(p,k;E_R)Y_{lm_l}(\hat{p})|m_s\rangle\langle m'_s|Y^*_{lm'_l}(\hat{k}). \tag{21}$$

This expansion should not be confused with the sum in Eq. (20): each lj term contributes to the hadronic tensor and can come either from a quasihole state or from above the Fermi surface, depending on the excitation energy.

The angular integrations in Eq. (19) can be easily performed by noting that the square root of the Darwin nonlocality factor, $D^{\pm 1/2}(r)$ in Eq. (13), is not far from 1, which would yield $\delta(\vec{p}\,'-\vec{p}-\vec{q})$ in momentum space (see Fig. 1 in the next Sec. III B). Therefore, because of Eq. (17), we impose the constraint that the vector $\vec{p}$ in Eq. (19) lies in the same direction as $\vec{p}_f-\vec{q}$, i.e.,

$$\vec{p}\sim p\frac{\vec{p}_f-\vec{q}}{|\vec{p}_f-\vec{q}|}=\frac{p}{\sqrt{(\vec{p}\,'_N-\vec{q})^2+p_I^2}}(\vec{p}_f-\vec{q}), \tag{22}$$

and similarly for $\vec{k}$. This approximation is reliable for high values of the involved momenta, as is the case for the kinematics of Ref. [19]. It is then easy to get rid of the angular integrations in Eq. (19) so that the hadronic tensor, with explicit spin quantum numbers, takes the form

$$(W_{\lambda,\lambda'})_{s'_N}=(-1)^{\lambda+\lambda'}e^{\mu}_{\lambda}e^{\nu *}_{\lambda'}e^{-2\vec{p}_I\cdot\vec{R}}\sum_{lj}\sum_{m_l,m'_l}\sum_{m_s,m'_s}(l\tfrac{1}{2}\,m_l m_s|jm)(l\tfrac{1}{2}\,m'_l m'_s|jm)Y_{lm_l}(\widehat{p_f-q})Y^*_{lm'_l}(\widehat{p_f-q})$$

$$\times\int_0^\infty dp\,p^2\int_0^\infty dk\,k^2\langle s'_N|(\hat{J}_{\rm eff})_\mu(p,\vec{p}_f,\vec{q},\omega)|m_s\rangle S_{lj}(p,k;E_R)\langle m'_s|(\hat{J}_{\rm eff})^\dagger_\nu(k,\vec{p}_f,\vec{q},\omega)|s'_N\rangle, \tag{23}$$

where $\hat{J}^\mu_{\rm eff}(p,\vec{p}_f,\vec{q},\omega)$ is defined by inserting approximation (22) into Eq. (18).

Since the missing energy of the reaction is defined as [11,13]

$$E_m=\omega-T_{p'_N}-T_R, \tag{24}$$

where $T_{p'_N}$ is the kinetic energy of the detected nucleon and

$$T_R=[p_m^2+(M_R+E_R)^2]^{1/2}-M_R-E_R \tag{25}$$

is the kinetic energy of the residual nucleus, the scattering amplitude $J^\mu_{s'_N n}(\omega,\vec{q},\vec{p}\,'_N,E_R)$ of Eq. (18) can be conveniently made to depend on $(\omega,\vec{q},\vec{p}_m,E_m)$. Therefore, the differential cross section (and other related observables) for a given kinematics $(\omega,\vec{q})$ and a knockout proton corresponding to a missing energy E_m will be plotted as a function of the missing momentum $\vec{p}_m$. Older experimental $(e,e'p)$ data at low proton energy were usually collected in the form of the so-called reduced cross section [10,11]

$$n(\vec{p}_m,E_m)\equiv\frac{d\sigma}{d\vec{p}\,'_e d\vec{p}\,'_N}\frac{1}{K\sigma_{eN}}, \tag{26}$$

where K is a suitable kinematic factor and σ_{eN} is the elementary (half off-shell) electron-nucleon cross section, in order to reduce the information contained in a fivefold differential

cross section to a twofold function of $\vec{p}_m$ and E_m. Whenever needed, theoretical results will also be presented as reduced cross sections using the CC1 prescription [17] for σ_{eN} and the corresponding extrapolation $\overline{\omega}=E'_N-\overline{E}$ (with $\overline{E}=\sqrt{p_m^2+m^2}$) for the off-shell nucleon. The electron distortion is included in the EMA by replacing $\vec{q}$ with an effective $\vec{q}_{\rm eff}$ [47] for the acceleration by the Coulomb field (in the following, for sake of simplicity the subscript eff will be omitted).

III. QUASIHOLE AND QUASIPARTICLE PROPERTIES

The calculation of the $(e,e'p)$ cross section is most easily performed by employing the quasihole wave function of Eq. (5). By considering Eq. (21) in a SP basis with orbital angular momentum l, total angular momentum j, and momentum p, we can relate the spectroscopic amplitude to the spectral function in the following way:

$$S_{lj}(p,k;E)=\sum_n \langle\Psi_0^{\rm A}|a_{klj}^\dagger|\Psi_n^{\rm A-1}\rangle\langle\Psi_n^{\rm A-1}|a_{plj}|\Psi_0^{\rm A}\rangle \times\delta(E-(E_0^A-E_n^{A-1})), \tag{27}$$

where a_{plj} ($a_{klj}^\dagger$) denotes the removal (addition) operator for a nucleon. The spectral function $S_{lj}(p,k;E)$ can be obtained from the imaginary part of the corresponding SP propagator $g_{lj}(p,k;E)$. This Green's function solves the Dyson equation

$$g_{lj}(p,k;E)=g_{lj}^{(0)}(p,k;E)+\int dp_1p_1^2\int dp_2p_2^2g_{lj}^{(0)}(p,p_1;E) \times\Delta\Sigma_{lj}(p_1,p_2;E)g_{lj}(p_2,k;E), \tag{28}$$

where $g^{(0)}$ refers to a Hartree-Fock propagator and $\Delta\Sigma_{lj}$ represents contributions to the real and imaginary parts of the irreducible self-energy, which go beyond the Hartree-Fock approximation of the nucleon self-energy used to derive $g^{(0)}$ (see below). A brief summary of the calculation of the self-energy and the solution of the Dyson equation are included below. More details can be found in Refs. [29,48].

A. Quasihole properties

The self-energy is constructed by a two-step approach employing the boson-exchange potential B as defined by Machleidt in Ref. [49]. The treatment of short-range correlations is taken into account by solving the Bethe-Goldstone equation. In the first step this equation is solved in nuclear matter at a certain density with a reasonable choice for the starting energy. Employing a vector bracket transformation [50], the corresponding ''Hartree-Fock'' self-energy contribution in momentum space is calculated for ^{16}O using harmonic oscillator wave functions for the occupied states with oscillator length $\alpha=1.72$ fm^{-1}. Since this ''Hartree-Fock'' self-energy is obtained from nuclear matter, corrections need to be applied to reinstate the properties of the ^{16}O Fermi surface. In addition, higher-order self-energy contributions are included. This procedure involves the calculation of the imaginary part of the self-energy for two-particle–one-hole (2p1h) and two-hole–one-particle (2h1p) intermediate states reached by the G-matrix interaction and calculated in ^{16}O. The intermediate particle states correspond to plane waves and must be orthogonalized to the bound SP states [51]. Pure kinetic energies are assumed for these particle states. While this assumption is not very realistic for the description of the coupling to low-lying states, it is quite adequate for the treatment of tensor and short-range correlations. From these imaginary contributions to the self-energy one can obtain the corresponding real parts by employing the appropriate dispersion relations. Since the ''Hartree-Fock'' part was calculated in terms of a G matrix, it already contains the 2p1h contribution mentioned above but generated in nuclear matter. The corresponding real part of the self-energy as calculated in nuclear matter is then subtracted to eliminate the double counting terms. This procedure is quite insensitive to the original choice of density and starting energy for the nuclear matter G matrix [29,48]. For the determination of the p-shell quasihole wave functions only the real part of the self-energy is relevant. Collecting all the contributions to this self-energy one has

$$\begin{aligned}{\rm Re}\,\Sigma_{lj}(p,k;E)&=\Sigma_{lj}^{HF}(p,k)+{\rm Re}\,\Sigma_{lj}^{\rm 2p1h}(p,k;E)\\&\quad-{\rm Re}\,\Sigma_{lj}^{c}(p,k;E)+{\rm Re}\,\Sigma_{lj}^{\rm 2h1p}(p,k;E)\\&=\Sigma_{lj}^{HF}(p,k)+{\rm Re}\,\Delta\Sigma_{lj}(p,k;E),\end{aligned} \tag{29}$$

with obvious notation. In the last line of Eq. (29) we have included (the real part of) $\Delta\Sigma_{lj}$, which was anticipated in Eq. (28). This self-energy yields a complete treatment of the effect of short-range and tensor correlations for a finite nucleus [52]. The resulting wave functions for p-shell nucleons also yield an excellent description of the shape of the experimental $(e,e'p)$ cross section [30]. The self-energy in Eq. (29) does not include an adequate description of the coupling of the nucleon to low-lying collective excitations that strongly influence the spectroscopic factors [53–55]. This deficiency is not important for the present paper since we are addressing the question of the reliable extraction of spectroscopic factors from $(e,e'p)$ data. It is therefore of great importance that the theoretical wave functions generated by Eq. (29) are of equivalent quality to the empirical ones used in the analysis of the data [31]. Indeed, when these wave functions are used to fit the data [30], they yield spectroscopic factors that are essentially identical to the ones from the empirical analysis.

The solution of the Dyson equation was previously obtained in a basis generated by enclosing the system in a spherical box [29,48]. For the present paper the Dyson equation has been solved directly in momentum space by performing the discretization for the relevant eigenvalue problem. For discrete solutions such as the quasihole states in ^{16}O, the Dyson equation yields the following eigenvalue equation:

$$\frac{p^2}{2m}\langle\Psi_n^{A-1}|a_{plj}|\Psi_0^A\rangle+\int_0^\infty dk k^2 \mathrm{Re}\,\Sigma_{lj}(p,k;E_n)$$
$$\times\langle\Psi_n^{A-1}|a_{klj}|\Psi_0^A\rangle=E_n\langle\Psi_n^{A-1}|a_{plj}|\Psi_0^A\rangle. \quad (30)$$

Discretizing the integration in Eq. (30) yields a straightforward diagonalization problem. The resulting quasihole wave functions for the $p_{1/2}$ and $p_{3/2}$ states are used for the analysis presented in Sec. IV. We have checked that the present solution method yields identical results as compared to those from the ''box method.''

B. Darwin nonlocality factor

As discussed in Sec. II A, the Darwin nonlocality factor given by Eq. (7) is required for a proper treatment of the current operator at high proton energies. It is clear from Eq. (8) that this nonlocality factor is related to the spin-orbit potential. This relation can therefore be used to derive the nonlocality factor from the nucleon self-energy discussed in Sec. III A. A complication in deriving this result is that the self-energies constructed for ^{16}O are inherently nonlocal in coordinate space. This many-body nonlocality is already present when Fock terms to the self-energy are considered. Additional contributions are generated when higher-order terms are included as in Eq. (29). The terminology here may be confusing so it is useful to point out that the Darwin nonlocality factor refers to the nonrelativistic reduction of the Dirac equation, which yields a nonlocal term in the Schrödinger equation when starting from a local Dirac equation.

Since Eq. (8) requires a local spin-orbit potential we will construct local potentials from the nonlocal self-energies. As shown in Ref. [51], it is possible to construct local potentials from the nonlocal self-energy by using the following expression:

$$\mathrm{Re}\,\Sigma_{lj}^{local}(r)=\int_0^\infty dr' r'^2 \mathrm{Re}\,\Sigma_{lj}(r,r';E), \quad (31)$$

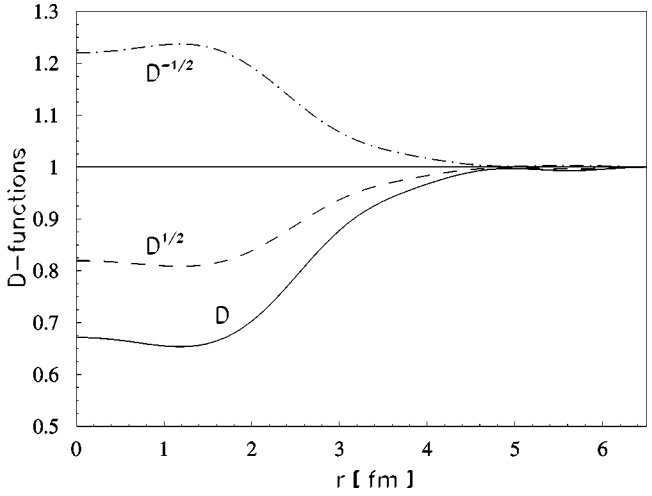

FIG. 1. The Darwin nonlocality factor $D(r)$ obtained by inverting Eq. (8). Dashed and dot-dashed lines show $D^{1/2}(r)$ and $D^{-1/2}(r)$ entering Eq. (13), respectively.

where the nonlocal self-energy in coordinate space is obtained from the one in momentum space by a double Fourier-Bessel transformation given by

$$\mathrm{Re}\,\Sigma_{lj}(r,r';E)=\frac{2}{\pi}\int_0^\infty dp p^2\int_0^\infty dp' p'^2 j_l(pr)$$
$$\times \mathrm{Re}\,\Sigma_{lj}(p,p';E) j_l(p'r'). \quad (32)$$

As shown in Ref. [51], a good representation to local potentials given by Eq. (31) is generated by a Woods-Saxon form. Following this procedure we have obtained two local Woods-Saxon potentials $V_{p_{1/2}}(r)$ and $V_{p_{3/2}}(r)$ for the relevant p-shell quasihole states in ^{16}O, respectively. Since the goal of the present work is to study the possibility to extract spectroscopic factors at different Q^2, we have adjusted these potentials slightly to generate the correct experimental spin-orbit splitting. In addition, we have ensured that the corresponding wave functions in momentum space have the maximum overlap with those of the nonlocal self-energies. These overlaps are given by 99.97% for the $p_{1/2}$ and 99.99% for the $p_{3/2}$ wave functions, respectively. It is now possible to decompose the local potentials $V_{p_{1/2}}$ and $V_{p_{3/2}}$ in central and spin-orbit potentials in the following way:

$$V=U_0+U_{LS}\vec{L}\cdot\vec{S}. \quad (33)$$

For p states this implies that

$$U_{LS}(r)=\frac{2}{3}[V_{p_{3/2}}(r)-V_{p_{1/2}}(r)]. \quad (34)$$

This potential can then be used to construct the Darwin nonlocality factor by inverting Eq. (8). The latter is displayed in Fig. 1 together with the functions $D^{\pm 1/2}(r)$ used in Eq. (13). The observed small deviation from unity of the latter functions is the basis for the approximation introduced in Eq. (22) leading to the hadron tensor (23).

C. Damping of a quasiparticle

As discussed in Sec. II B, we will assume that the damping of the nucleon on its way out of the nucleus is described by a corresponding process taking place in nuclear matter. Since the SP momentum is conserved in nuclear matter, the propagation of a nucleon through nuclear matter is diagonal in the SP momentum and can be represented by

$$g(p;E)=\int_{\epsilon_F}^\infty d\omega \frac{S_\mathrm{p}(p;\omega)}{E-\omega+i\eta}+\int_{-\infty}^{\epsilon_F} d\omega \frac{S_\mathrm{h}(p;\omega)}{E-\omega-i\eta}, \quad (35)$$

where S_p and S_h (particle and hole spectral function) describe the strength distribution above and below the Fermi energy for a nucleon with SP momentum p. These spectral functions have recently been determined self-consistently by including the effects of short-range and tensor correlations in the self-energy [28]. For this purpose the effective interaction is represented by the equivalent of the T matrix in the medium [56,57]. The propagation of the nucleons determining this in-medium interaction is also described by Eq. (35), which

includes full off-shell effects. The resulting interaction is employed to construct the nucleon self-energy. This self-energy is then used to solve the Dyson equation for nuclear matter:

$$g(p;E)=g^{(0)}(p;E)+g^{(0)}(p;E)\Sigma^{NM}(p;E)g(p;E), \tag{36}$$

where the unperturbed propagator is given by

$$g^{(0)}(p;E)=\frac{\theta(p-p_F)}{E-p^2/2m+i\eta}+\frac{\theta(p_F-p)}{E-p^2/2m-i\eta}. \tag{37}$$

The solution procedure for this problem involves several iteration steps that are required because the solution to the Dyson equation already appears in the determination of the effective interaction and the self-energy, illustrating the nonlinearity of this problem. The solution of Eq. (36) can be written as

$$g(p;E)=\frac{1}{E-p^2/2m-\Sigma(p;E)}. \tag{38}$$

Taking advantage of the slow variation of the imaginary part of the self-energy as a function of p, one can expand the self-energy at the momentum p_0 for which

$$E\equiv\frac{p_0^2}{2m}+\mathrm{Re}\,\Sigma^{NM}(p_0;E). \tag{39}$$

Performing the expansion in the square of this momentum and keeping both real and imaginary parts of the self-energy at p_0 plus the first derivative of the real part, one obtains the so-called complex pole approximation (CPA) [56] for the propagator, which gives a very accurate representation of this quantity when transformed to coordinate space. For momenta above the Fermi momentum one has

$$g_{CPA}(p;E)=\frac{c_{p_0}}{p_0^2-p^2+i\gamma}, \tag{40}$$

where

$$c_{p_0}=\left(\frac{1}{2m}+\left.\frac{\partial\,\mathrm{Re}\,\Sigma^{NM}}{\partial p^2}\right|_{p_0^2}\right)^{-1} \tag{41}$$

and

$$\gamma=|\mathrm{Im}\,\Sigma^{NM}(p_0;E)|\left(\frac{1}{2m}+\left.\frac{\partial\,\mathrm{Re}\,\Sigma^{NM}}{\partial p^2}\right|_{p_0^2}\right)^{-1}. \tag{42}$$

This form of the propagator at a fixed energy has a simple pole structure in the complex momentum plane. The location of the relevant pole is given by

$$\kappa_0=(p_0^4+\gamma^2)^{1/4}e^{(i/2)\arctan(\gamma/p_0^2)}. \tag{43}$$

The imaginary part of this momentum is then used to describe the damping in the eikonal approximation described in Sec. II B, i.e., Im $\kappa_0\equiv p_{\mathrm{I}}$, with p_{I} from Eq. (15). To clarify the physics further one may obtain the propagator in coordinate space using

$$g_{CPA}(\vec{r},\vec{r}';E)=\frac{1}{(2\pi)^3}\int d^3p\,e^{i\vec{p}\cdot(\vec{r}-\vec{r}')}g_{CPA}(p;E)$$
$$=-\frac{c_{p_0}}{4\pi}\frac{e^{i\kappa_0|\vec{r}-\vec{r}'|}}{|\vec{r}-\vec{r}'|}. \tag{44}$$

From this result it is clear that the damping of the nucleon propagating through nuclear matter is determined by the imaginary part of κ_0, which in turn is determined by the imaginary part of the self-energy at this energy. In Fig. 2 the quantity γ of Eq. (42), related to the imaginary part of the self-energy, is shown as a function of $p_0\sim\mathrm{Re}\,\kappa_0\equiv p_N'$. It is remarkable that at $p_N'\sim 7$ fm^{-1}, i.e., at the same proton kinematics of the NE18 experiment [36], γ is such that Im $\kappa_0\equiv p_{\mathrm{I}}\sim 50$ MeV/c gives the proper damping necessary to describe the observed absorption. In fact, in the context of the pure Glauber approximation ($W\propto p_N'$) one would expect a higher proportionality factor, thus overestimating the quenching due to FSI (see Ref. [27] and references therein). The outlined derivation of γ gives a microscopic explanation for reducing this proportionality factor when embedding the traveling proton in nuclear matter.

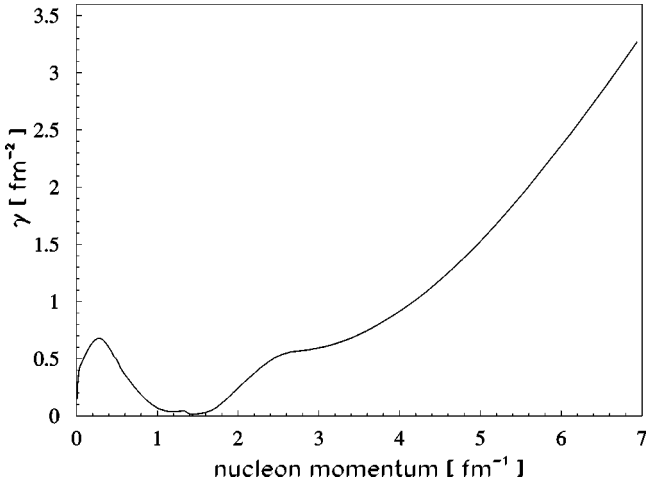

FIG. 2. The quantity γ of Eq. (42), related to the imaginary part of the nucleon self-energy, as function of $p_0\sim p_N'$, the nucleon momentum.

This absorption effect of the medium is obtained for a realistic nucleon-nucleon interaction [58]. Since this interaction is fitted to low-energy data, it is used in the Lippmann-Schwinger equation to describe these data. As a result, the coupling to intermediate states at higher energy is constrained by the fit to these low-energy data. Whether the description of these intermediate states as nonrelativistic two-nucleon states is accurate is then less relevant. One may also interpret the coupling to these intermediate (nonrelativistic two-nucleon) states as a phenomenological way to include the coupling to inelastic channels, quark effects, etc. For this reason we expect the present microscopic descrip-

tion of nucleon absorption in the medium to be fully relevant for the $(e,e'p)$ reactions studied in this paper. Since quite different nucleon-nucleon interactions are capable of fitting the low-energy data, it may be instructive to explore the dependence of the imaginary part of the self-energy in the relevant energy and momentum domain on the chosen interaction. At this time we have only self-consistent calculations for the Reid potential available. We certainly plan to extend our self-consistent calculations to other interactions in order to study this issue in more detail in the future (see also Ref. [59]). One may then employ a possible sensitivity to the chosen interaction as a means to identify those interactions that have the proper behavior when in-medium properties are considered.

IV. RESULTS

In this section we will discuss the results for the cross section of the $^{16}O(e,e'p)$ reaction leading to the ground state and the first $\frac{3}{2}^-$ excited state of the residual ^{15}N nucleus. The main theoretical ingredient is the hadronic tensor of Eq. (23), which describes the electromagnetic interaction assuming a relativistic one-body current operator including spinor distortion in the initial state only. This is consistent with the spin-orbit effects associated with the quasihole states in the residual nucleus [see Eq. (8)]. The proton scattering wave is described in the eikonal approximation (EA), assuming a uniform and constant damping by nuclear matter through a nucleon self-energy containing the same short-range correlations used to generate the properties of the quasihole in the bound state. The electron wave is described through the EMA, which incorporates the acceleration due to the Coulomb field.

We first reconsider this reaction at low Q^2 using the conventional optical potential analysis for FSI [30]. In Fig. 3 the data from Ref. [31] have been collected at a constant proton energy of 90 MeV in the center-of-mass system. They refer to the reduced cross section, defined by Eq. (26), as a function of the missing momentum p_m in parallel kinematics, i.e. for $\vec{p}'_N \| \vec{q}$. Therefore, the p_m distribution can be obtained by increasing the momentum transfer q from positive to negative values of p_m. Two transitions were considered, leading to the ground state $p_{1/2}$ and to the first excited state $p_{3/2}$ at $E_m = 6.32$ MeV of ^{15}N. The data for the transition to the $p_{1/2}$ ground state have been multiplied by 20. The solid lines are the result of the calculation employing the quasihole part of the spectral function of Eq. (21) for the $p_{1/2}$ and $p_{3/2}$ partial waves, respectively. The normalization of the curves is adjusted to fit the data, indicating that the intrinsic normalization of the quasihole, 0.89 for the $p_{1/2}$ and 0.914 for the $p_{3/2}$, must be significantly reduced to $Z_{0p_{1/2}} = 0.644$ and $Z_{0p_{3/2}} = 0.537$, respectively, because only the depletion due to short-range correlations has been taken into account [30]. Incidentally, long-range correlations spread the total $\frac{3}{2}^-$ strength over three states in the discrete spectrum, so that the $p_{3/2}$ data account for 86% of the strength only; by rescaling the spectroscopic factor by this fraction we get $Z_{0p_{3/2}} = 0.624$, in close agreement with the corresponding ground-state value [30]. The dashed lines in Fig. 3 refer to the calculation including the same spectroscopic factors but replacing the quasihole bound state by the wave function of Ref. [60], which is obtained by a Skyrme-Hartree-Fock method for ^{16}O. Both descriptions are in very good agreement with the data, with a slight preference for the quasihole results at negative p_m.

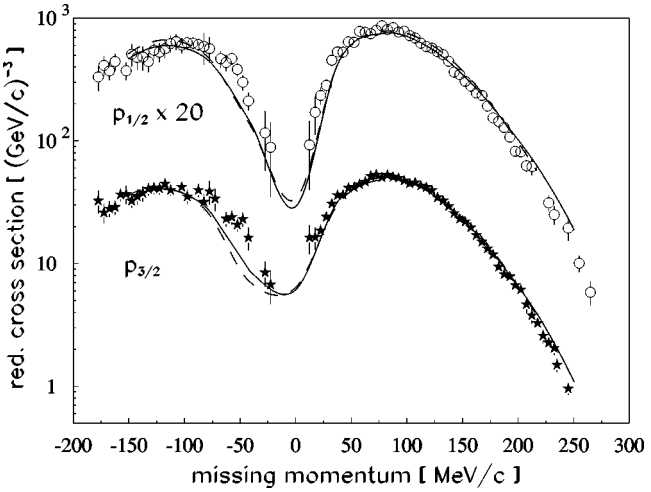

FIG. 3. Cross section for the $^{16}O(e,e'p)^{15}N$ reaction at $E_p = 90$ MeV constant proton energy in the center-of-mass system in parallel kinematics [31]. Data for the $p_{1/2}$ state have been multiplied by 20. Solid line is the result of Ref. [30] using quasihole states; dashed line represents the same result but replacing the quasihole spectral function with the bound state from Ref. [60]. All curves have been rescaled by the spectroscopic factors $Z = 0.644$ and $Z = 0.537$ for the $p_{1/2}$ and $p_{3/2}$ states, respectively.

In Fig. 4 the same reaction is considered in a very different kinematical regime, namely at constant $(\vec{q},\omega)$ with $Q^2 = 0.8$ $(\mathrm{GeV}/c)^2$ [19]. The data here refer to a fivefold differential cross section, avoiding any ambiguity in modeling the half off-shell elementary cross section σ_{ep} of Eq. (26). Again, results for the transition to the ground state $p_{1/2}$ have been multiplied by 20. The theoretical calculations are displayed with the same notation as in Fig. 3, i.e., solid lines for the results with the quasihole bound state and dashed lines by employing the wave function of Ref. [60]. The preference for the first choice is here more evident. In any case, it is remarkable that the calculations reproduce the data by using the same spectroscopic factors as in the previous kinematics, i.e., $Z_{0p_{1/2}} = 0.644$ and $Z_{0p_{3/2}} = 0.537$. Therefore, contrary to the findings of Ref. [16], we do not find any need for a Q^2 dependence of the spectroscopic factors over a wide kinematical range, in agreement also with the results obtained by a mean-field description in the context of relativistic DWIA [61]. This outcome is particularly welcome, since by definition these factors describe a spectroscopic nuclear property that must be independent of the probe scale Q^2. Finally, we conclude that the treatment of the bound-state wave function is not responsible for the Q^2 dependence found in Ref. [16]. From this observation one may infer that it is useful to extend the analysis of the high-Q^2 data to other nuclei using the eikonal description supplemented with the nuclear matter

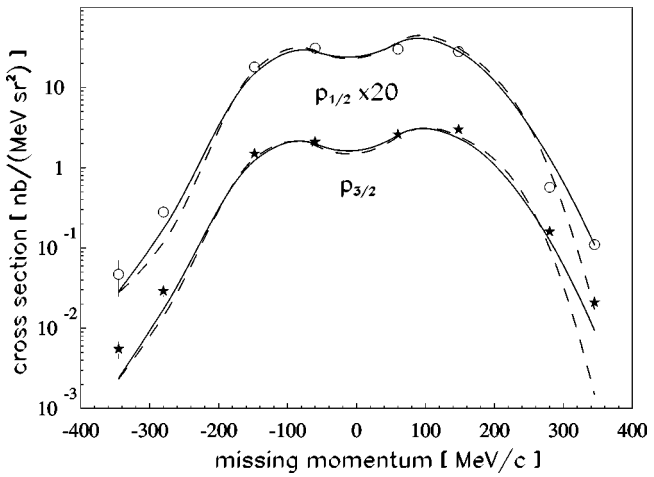

FIG. 4. Cross section for the $^{16}\mathrm{O}(e,e'p)^{15}\mathrm{N}$ reaction at $Q^2=0.8$ $(\mathrm{GeV}/c)^2$ in perpendicular kinematics [19]. Data for the $p_{1/2}$ state have been multiplied by 20. The solid lines represent the result of the present calculation. The dashed lines are obtained by replacing the quasihole states with the bound-state wave functions of Ref. [60]. In all cases, the results have been rescaled by the same spectroscopic factors as in Fig. 3, namely $Z=0.644$ and $Z=0.537$ for the $p_{1/2}$ and $p_{3/2}$ states, respectively.

damping description while foregoing the use of microscopic quasihole wave functions. Clearly an analysis of the data considered in Refs. [15,16] will further clarify the validity of the present analysis. It is already encouraging to note that the damping obtained in our calculations is adequate to describe the observed absorption in the NE18 experiment [36] as discussed in Sec. III C.

In Fig. 5 we show the results for the structure functions

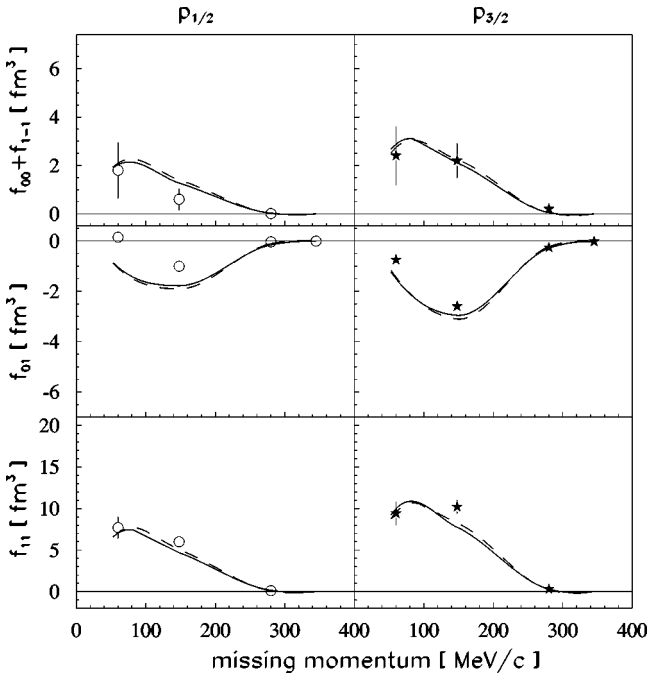

FIG. 5. Structure functions for the $^{16}\mathrm{O}(e,e'p)^{15}\mathrm{N}$ reaction at $Q^2=0.8$ $(\mathrm{GeV}/c)^2$ in perpendicular kinematics [19]. The same notation and scaling of curves are used as in Fig. 4.

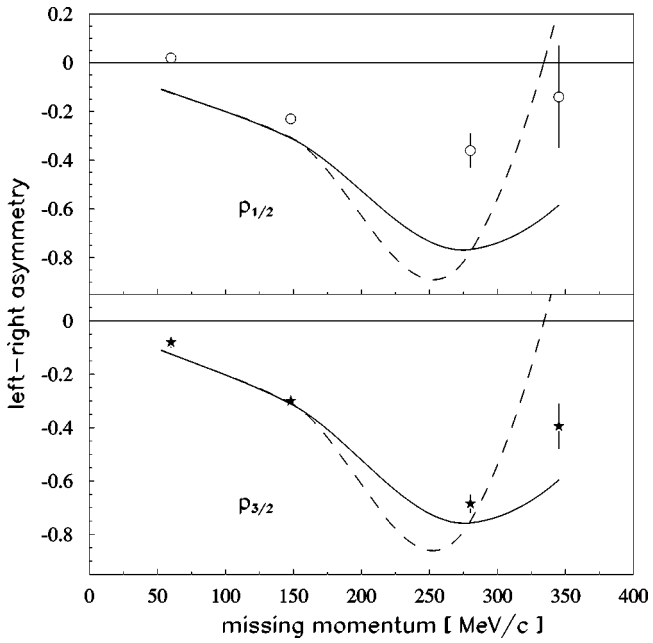

FIG. 6. Left-right asymmetry for the $^{16}\mathrm{O}(e,e'p)^{15}\mathrm{N}$ reaction at $Q^2=0.8$ $(\mathrm{GeV}/c)^2$ in perpendicular kinematics [19]. The same notation is used as in Fig. 4.

$f_{\lambda,\lambda'}$ in the same kinematics and with the same notation as in Fig. 4. They are defined by

$$f_{00}=W'_{00},$$

$$f_{11}=W'_{11}+W'_{-1-1},$$

$$f_{01}=2\,\mathrm{Re}[W'_{01}-W'_{0-1}],$$

$$f_{1-1}=2\,\mathrm{Re}[W'_{1-1}], \tag{45}$$

with $W'_{\lambda,\lambda'}$ the hadronic tensor in the proton center-of-mass system. It is related to $W_{\lambda,\lambda'}$ in the laboratory frame by the transformation $W_{\lambda,\lambda'}=e^{i\alpha(\lambda-\lambda')}W'_{\lambda,\lambda'}$, i.e., by a rotation around the $\vec{q}$ direction of the angle α between the lepton scattering plane and the plane formed by $\vec{q}$ and $\vec{p}'_N$. The rotation affects only the interference components, so that the cross section (1) becomes [10,11]

$$\frac{d\sigma}{d\vec{p}'_e d\vec{p}'_N}=\frac{e^4}{16\pi^2}\frac{1}{Q^4 p_e p'_e}\{L_{00}f_{00}+L_{11}f_{11} +L_{01}f_{01}\cos\alpha+L_{1-1}f_{1-1}\cos 2\alpha\}, \tag{46}$$

i.e., it becomes parametrized in terms of the different components of the nuclear response $f_{\lambda,\lambda'}$ to the virtual photon probe in the spherical basis. The agreement with data is still good for both transitions over the whole p_m range, except for f_{01}, the interference between the longitudinal and transverse responses, which is known to be particularly sensitive to relativistic effects [21,62,63].

Correspondingly, the left-right asymmetry

$$A_{LT}=\frac{d\sigma(\alpha=0°)-d\sigma(\alpha=180°)}{d\sigma(\alpha=0°)+d\sigma(\alpha=180°)} \tag{47}$$

is displayed in Fig. 6 under the same conditions and with the same notation as in Fig. 4. The discrepancy previously noted for f_{01} is amplified here, particularly for the results with the bound state of Ref. [60]. A possible explanation is that only a full account of relativistic effects, specifically of spinor distortion in both bound and scattering states, is needed to reproduce the data [19,21,62]. In the present calculation this effect is included only for the bound state, while the Darwin nonlocality factor for the scattering state turns out to be 1 because the homogeneous damping in nuclear matter does not include spin-orbit contributions.

V. CONCLUSIONS

We have developed a model for describing the $(e,e'p)$ reaction at high Q^2 while linking it to nonrelativistic microscopic many-body ingredients such as the quasihole spectral function. The goal is to critically consider the issue raised in Refs. [15,16] about a possible dependence of the spectroscopic factors upon Q^2.

We use an unfactorized approach where, following Ref. [21], a relativistic one-body electromagnetic current operator is adopted in a Schrödinger-based framework avoiding any nonrelativistic reduction. The effect of spinor distortion by the Dirac scalar and vector potentials is consistently included only for the bound state by evaluating the Darwin nonlocality factor through the spin-orbit potential generated by the self-energy of the quasihole spectral functions. The proton scattering wave is described in an eikonal approximation (tested against DWIA solutions of a complex spin-dependent optical potential [26]). The absorption is calculated by using a spectral function for nucleons in nuclear matter including the same short-range and tensor correlations adopted in the calculation of the nucleon self-energy in a finite volume for the p-shell quasihole states of ^{16}O.

In Ref. [30] these bound-state wave functions have been used to analyze the data for $^{16}\mathrm{O}(e,e'p)$ at low Q^2 [31], yielding a very good description of the reduced cross sections. In the present work, we have considered the recent data for the same reaction at higher Q^2 [19] and we have performed the analysis using the same bound-state wave functions and the same spectroscopic factors extracted from the low-Q^2 analysis. The description of the data at higher Q^2 is still very good regarding both the fivefold differential cross section and the structure functions. Only the interference f_{01} structure function, and the related left-right asymmetry A_{LT}, show a visible discrepancy, particularly for the $p_{1/2}$ state. A possible explanation could be related to our incomplete treatment of the relativistic effects because the spinor distortion of the final state is not considered.

However, we emphasize that our consistent analysis of low- and high-Q^2 data using the same microscopic many-body ingredients for the quasihole states and the damping of the proton scattering wave allow us to conclude that we do not observe any Q^2 dependence of the spectroscopic factors over the considered wide range $0.02\leqslant Q^2\leqslant 0.8$ $(\mathrm{GeV}/c)^2$. This outcome is most welcome, since by definition these factors describe a spectroscopic nuclear property that must be independent of the probe scale Q^2. Finally, since we get a very good description of the high-Q^2 data replacing our quasihole states with the bound states of Ref. [60], we can also conclude that the quality of the wave functions is not responsible for the unexpected Q^2 dependence of the spectroscopic factors observed in Ref. [16].

ACKNOWLEDGMENTS

This work is supported by the U.S. National Science Foundation under Grant No. PHY-9900713. We acknowledge the hospitality of the Laboratory of Theoretical Physics at University of Gent, where part of this work was done.

[1] A.E.L. Dieperink and P.K.A. de Witt Huberts, Annu. Rev. Nucl. Part. Sci. **40**, 239 (1990).
[2] I. Sick and P.K.A. de Witt Huberts, Comments Nucl. Part. Phys. **20**, 177 (1991).
[3] L. Lapikás, Nucl. Phys. **A553**, 297c (1993).
[4] V.R. Pandharipande, I. Sick, and P.K.A de Witt Huberts, Rev. Mod. Phys. **69**, 981 (1997).
[5] B.E. Vonderfecht, W.H. Dickhoff, A. Polls, and A. Ramos, Phys. Rev. C **44**, R1265 (1991).
[6] W.H. Dickhoff and H. Müther, Rep. Prog. Phys. **55**, 1947 (1992).
[7] W.H. Dickhoff, in *Nuclear Methods and the Nuclear Equation of State*, edited by M. Baldo (World Scientific, Singapore, 1999), p. 326.
[8] L. Lapikás (private communication).
[9] M.F. van Batenburg, Ph.D. thesis, University of Utrecht, 2001.
[10] S. Boffi, C. Giusti, and F.D. Pacati, Phys. Rep. **226**, 1 (1993).
[11] S. Boffi, C. Giusti, F.D. Pacati, and M. Radici, *Electromagnetic Response of Atomic Nuclei* (Oxford University Press, Oxford, 1996).
[12] J.J. Kelly, Adv. Nucl. Phys. **23**, 75 (1996).
[13] S. Frullani and J. Mougey, Adv. Nucl. Phys. **13**, 1 (1984).
[14] J.M. Udías, P. Sarriguen, E.M. de Guerra, E. Garrido, and J.A. Caballero, Phys. Rev. C **51**, 3246 (1995).
[15] L. Lapikás, G. van der Steenhoven, L. Frankfurt, M. Strikman, and M. Zhalov, Phys. Rev. C **61**, 064325 (2000).
[16] L. Frankfurt, M. Strikman, and M. Zhalov, Phys. Lett. B **503**, 73 (2001).
[17] T. de Forest, Nucl. Phys. **A392**, 232 (1983).
[18] J.M. Udías, J.A. Caballero, E. Moya de Guerra, J.R. Vignote, and A. Escuderos, Phys. Rev. C **64**, 024614 (2001).
[19] J. Gao *et al.*, Jefferson Lab Hall A Collaboration, Phys. Rev. Lett. **84**, 3265 (2000).
[20] S. Jeschonnek, Phys. Rev. C **63**, 034609 (2001).
[21] J.J. Kelly, Phys. Rev. C **60**, 044609 (1999).
[22] M. Hedayati-Poor, J.I. Johansson, and H.S. Sherif, Phys. Rev. C **51**, 2044 (1995).
[23] A. Picklesimer and J.W. van Orden, Phys. Rev. C **40**, 290 (1989).

[24] S. Boffi, C. Giusti, F.D. Pacati, and F. Cannata, Nuovo Cimento A **98**, 291 (1987).
[25] Y. Jin and D.S. Onley, Phys. Rev. C **50**, 377 (1994).
[26] A. Bianconi and M. Radici, Phys. Rev. C **56**, 1002 (1997).
[27] A. Bianconi and M. Radici, Phys. Rev. C **54**, 3117 (1996).
[28] E.P. Roth, Ph.D. thesis, Washington University, St. Louis, 2000.
[29] H. Müther, A. Polls, and W.H. Dickhoff, Phys. Rev. C **51**, 3040 (1995).
[30] A. Polls, M. Radici, S. Boffi, W.H. Dickhoff, and H. Müther, Phys. Rev. C **55**, 810 (1997).
[31] M. Leuschner *et al.*, Phys. Rev. C **49**, 955 (1994).
[32] W.H. Dickhoff, E.P. Roth, and M. Radici, in *Proceedings of the Vth Workshop on Electromagnetically Induced Two-Hadron Emission*, edited by P. Grabmayr *et al.* (University of Lund, Lund, 2001), p. 232.
[33] S. Boffi, F. Cannata, F. Capuzzi, C. Giusti, and F.D. Pacati, Nucl. Phys. **A379**, 509 (1982).
[34] S. Boffi and F. Capuzzi, Nucl. Phys. **A351**, 219 (1981).
[35] F.G. Perey, in *Direct Interactions and Nuclear Reaction Mechanism*, edited by E. Clementel and C. Villi (Gordon and Breach, New York, 1963), p. 125; F. Capuzzi, *Lecture Notes in Physics* (Springer-Verlag, Berlin, 1976), Vol. 55, p. 20.
[36] N.C.R. Makins *et al.*, NE18 Collaboration, Phys. Rev. Lett. **72**, 1986 (1994).
[37] T.G. O'Neill *et al.*, NE18 Collaboration, Phys. Lett. B **351**, 87 (1995).
[38] J.D. Bjorken and S.D. Drell, *Relativistic Quantum Mechanics* (McGraw-Hill, New York, 1964).
[39] P. Mergell, Ulf-G. Meissner, and D. Drechsel, Nucl. Phys. **A596**, 367 (1996).
[40] E.D. Cooper, S. Hama, B.C. Clark, and R.L. Mercer, Phys. Rev. C **47**, 297 (1993).
[41] R.J. Glauber, in *Lectures in Theoretical Physics*, edited by W. Brittain and L.G. Dunham (Interscience, New York, 1959), Vol. 1.
[42] C. Lechanoine-Leluc and F. Lehar, Rev. Mod. Phys. **65**, 47 (1993).
[43] A. Bianconi and M. Radici, Phys. Rev. C **53**, R563 (1996).
[44] G.D. Alkhazov, S.I. Belostotsky, and A.A. Vorobyev, Phys. Rep. **42**, 89 (1978).
[45] D. Debruyne, J. Ryckebusch, S. Janssen, and T. Van Cauteren, Phys. Lett. B **527**, 62 (2002).
[46] F. Cannata, J.P. Dedonder, and J.R. Gillespie, Nucl. Phys. **A467**, 636 (1987).
[47] C. Giusti and F.D. Pacati, Nucl. Phys. **A473**, 717 (1987); **A485**, 461 (1988).
[48] A. Polls, H. Müther, and W.H. Dickhoff, Nucl. Phys. **A594**, 117 (1995).
[49] R. Machleidt, Adv. Nucl. Phys. **19**, 1 (1989).
[50] C.W. Wong and D.M. Clement, Nucl. Phys. **A183**, 210 (1972).
[51] M. Borromeo, D. Bonatsos, H. Müther, and A. Polls, Nucl. Phys. **A539**, 189 (1992).
[52] H. Müther and W.H. Dickhoff, Phys. Rev. C **49**, R17 (1994).
[53] W.J.W. Geurts, K. Allaart, W.H. Dickhoff, and H. Müther, Phys. Rev. C **53**, 2207 (1996).
[54] C. Barbieri and W.H. Dickhoff, Phys. Rev. C **63**, 034313 (2001).
[55] C. Barbieri and W.H. Dickhoff, Phys. Rev. C **65**, 064313 (2002).
[56] W.H. Dickhoff, Phys. Rev. C **58**, 2807 (1998).
[57] W.H. Dickhoff, C.C. Gearhart, E.P. Roth, A. Polls, and A. Ramos, Phys. Rev. C **60**, 064319 (1999).
[58] R.V. Reid, Ann. Phys. (N.Y.) **50**, 411 (1968).
[59] Y. Dewulf, D. Van Neck, and M. Waroquier, Phys. Rev. C **65**, 054316 (2002).
[60] M. Zhalov (private communication).
[61] A. Meucci, C. Giusti, and F.D. Pacati, Phys. Rev. C **64**, 014604 (2001).
[62] J.M. Udías, J.A. Caballero, E. Moya de Guerra, J.E. Amaro, and T.W. Donnelly, Phys. Rev. Lett. **83**, 5451 (1999).
[63] D. Debruyne, J. Ryckebusch, W. Van Nespen, and S. Janssen, Phys. Rev. C **62**, 024611 (2000).